He et al., https://doi.org/10.1083/jcb.201701049

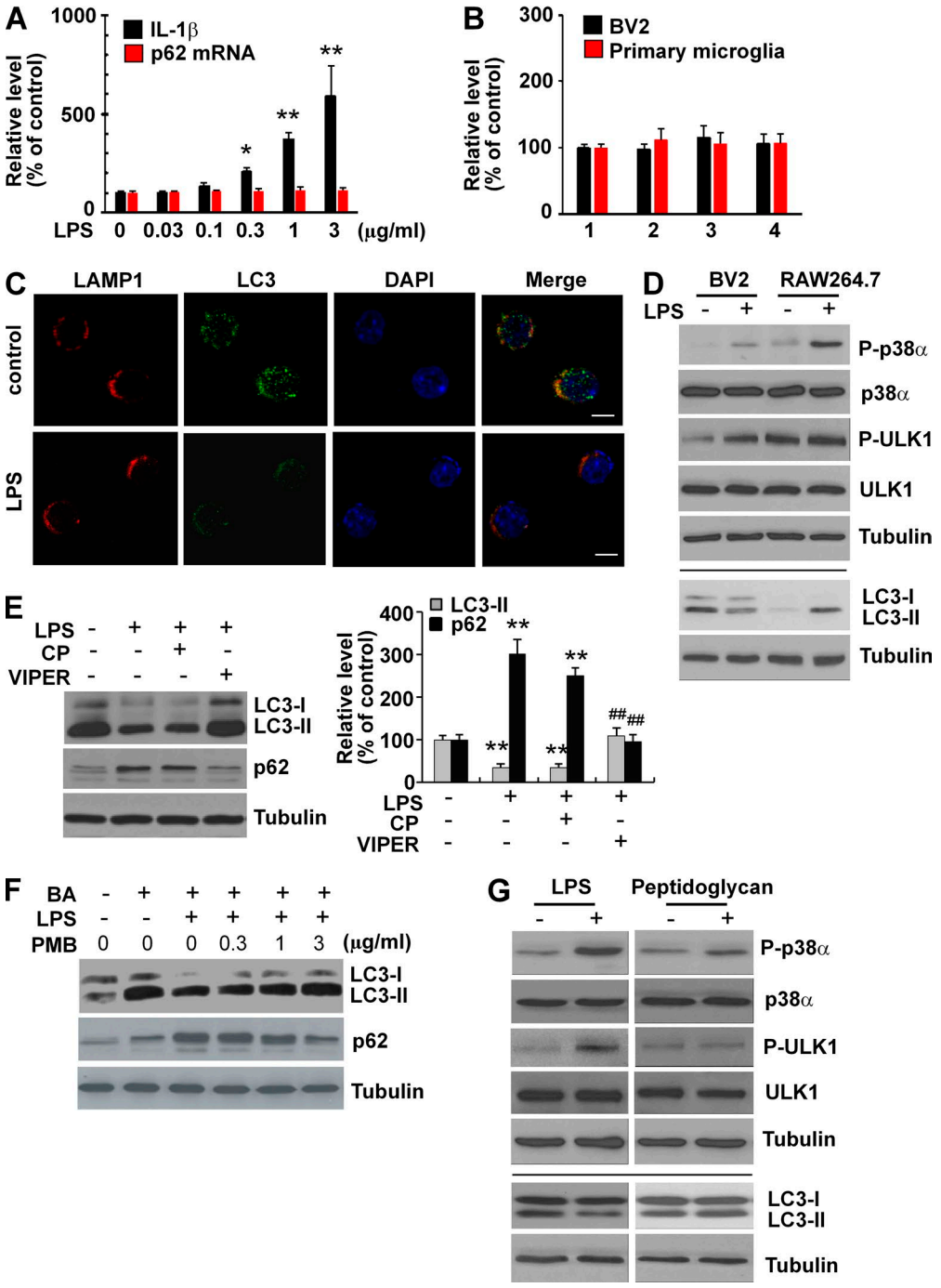

Figure S1. **LPS inhibits autophagy in microglia but not in RAW264.7 cells. (A)** Analysis of IL-1β in culture media by ELISA and of p62 mRNA in BV2 lysates by qRT-PCR after 8-h LPS treatment. **(B)** qRT-PCR analysis of p62 mRNA in BV2 cells and in primary microglia after rapamycin/LPS treatment as in Fig. 1 (D and E). **(C)** Reduction of the number of the LC3 and LAMP1 double-stained structure after LPS (1 µg/ml for 8 h) treatment in BV2 cells. Bars, 50 µm. **(D)** Different response of RAW264.7 cells to LPS. BV2 and RAW264.7 were treated with LPS (1 µg/ml) for 1 h (top) or 12 h (bottom) and blotted for various markers as shown. **(E)** Immunoblot analysis of extracts from BV2 cells treated with LPS (1 µg/ml for 8 h) in the presence of 5 µM VIPER, a TLR4-specific inhibiting peptide, or the control peptide (CP; 5 µM). **(F)** Immunoblot analysis of extracts from BV2 cells treated with LPS (1 µg/ml for 12 h) in the presence of BA (100 nM) and different concentrations of polymyxin B (PMB), an antibiotic that interferes with LPS–TLR4 binding. **(G)** Peptidoglycan (1 µg/ml), a TLR2 agonist, weakly activates p38α MAPK (1 h; top) and has no effect on LC3-II in BV2 cells (12 h; bottom). **, $P < 0.01$ versus control; ##, $P < 0.01$ versus LPS alone. $n = 4$. Error bars show SD.

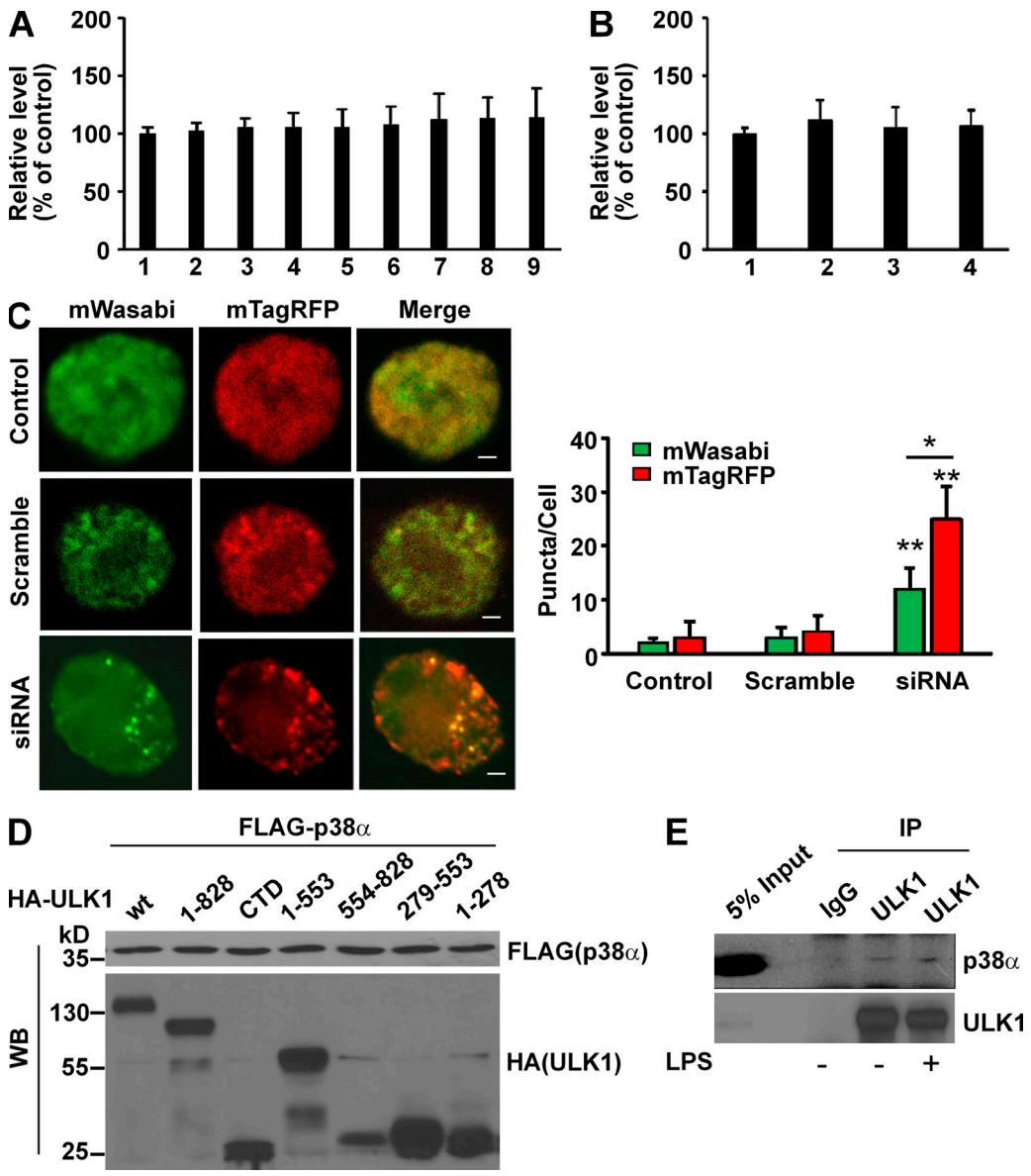

Figure S2. **LPS inhibits autophagy in BV2 cells through p38α MAPK. (A)** qRT-PCR analysis of p62 mRNA after LPS/SB203580 treatment as in Fig. 2 A. **(B)** qRT-PCR analysis of p62 mRNA after LPS/p38α knockdown as in Fig. 2 B. **(C)** Knockdown of p38α MAPK enhances autophagy in BV2 cells under basal conditions. Images were taken after BV2 cells were transfected with p38α siRNA and tandem-fluorescently tagged LC3 (mTagRFP-mWasabi-LC3) for 48 h. **(D)** HA-tagged WT ULK1 or ULK1 fragments were coexpressed with FLAG–p38α MAPK in HEK293 cells. CTD, C-terminal domain; WB, Western blot. **(E)** LPS (1 µg/ml) treatment has no effect on the ULK1–p38α MAPK interaction in BV2 cells. Co-IP was performed by incubating whole-cellular lysates (400 µg) with anti-ULK1 antibody. *, $P < 0.05$; **, $P < 0.01$ versus control. Bars 10 µm. $n = 100$. Experiments were repeated three times. Error bars show SD.

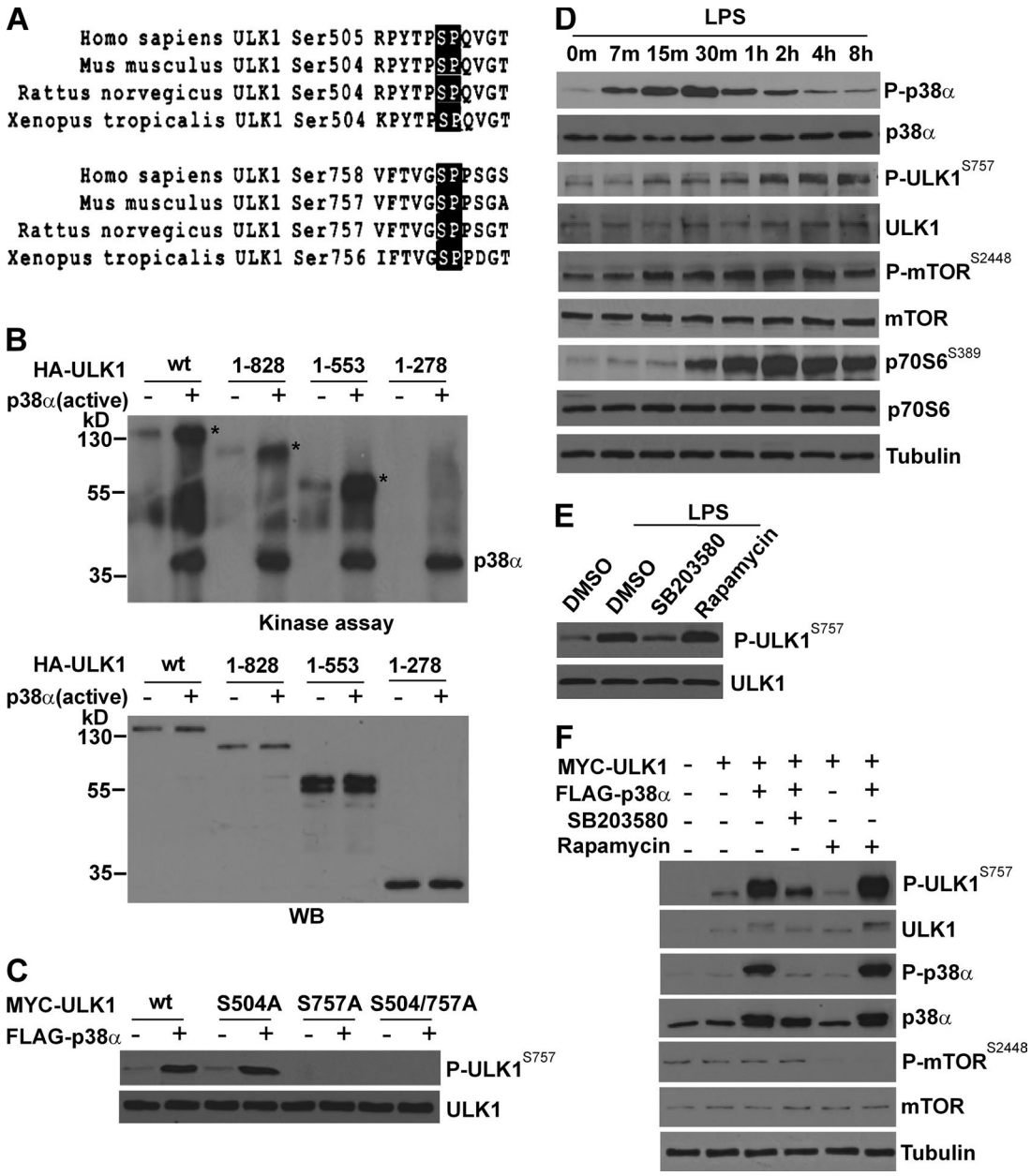

Figure S3. **p38α MAPK phosphorylates ULK1. (A)** Sequence alignment shows that serine 504 (S504) and serine *757* (S*757*) of ULK1 and the prolines followed are conserved among different species. **(B)** In vitro kinase assay showing the phosphorylation of various ULK1 fragments. ULK1 WT and fragments were immunoprecipitated from cellular lysates and incubated with an active recombinant p38α MAPK in a kinase assay. Asterisks denote phosphorylation signals. **(C)** Anti-ULK1^{S757} antibody specifically recognizes ULK1 when ULK1 is phosphorylated in vitro. WB, Western blot. **(D)** Activation of p38α MAPK precedes ULK1 phosphorylation after LPS treatment. BV2 cells treated with LPS (1 μg/ml) for various lengths of time were analyzed. **(E)** SB203580 but not rapamycin effectively blocks LPS-induced ULK1 phosphorylation at S*757*. BV2 cells were treated with LPS (1 μg/ml) and rapamycin (50 nM) or SB203580 (10 μM). **(F)** SB203580 but not rapamycin blocks p38α MAPK–induced ULK1 phosphorylation at S*757*. ULK1 and p38α MAPK were cotransfected into HEK293 cells. The cells were treated with SB203580 (10 μM) or rapamycin (50 nM) as indicated for 2 h.

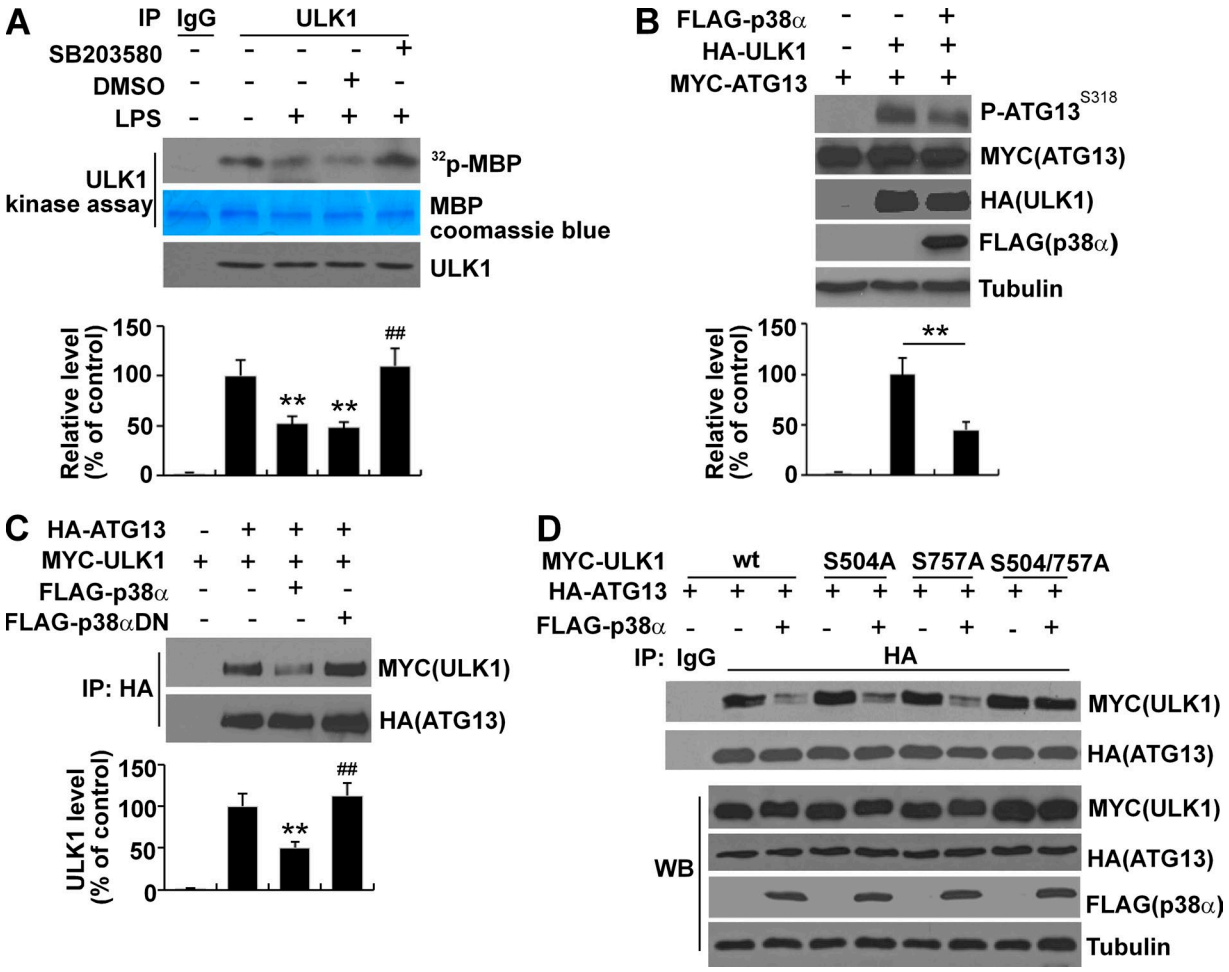

Figure S4. **p38α MAPK and inhibits ULK1 activity. (A)** SB203580 blocks LPS-induced inhibition of ULK1 kinase activity. BV2 cells were treated with LPS (1 µg/ml) with or without SB203580 (10 µM) for 2 h. ULK1 kinase activity was analyzed as described in Fig. 5 B. **(B)** Expression of p38α MAPK reduces the phosphorylation of ULK1 substrate ATG13. ATG13 and ULK1 were coexpressed with or without p38α MAPK in HEK293 for 24 h. Phosphorylation of ATG13 was determined by an anti–phospho ATG13^{S318} antibody. **(C)** Kinase-dead p38α MAPK (p38αDN) has no effect on the ULK1–ATG13 complex. ATG13 and ULK1 were coexpressed with p38α or p38αDN MAPK in HEK293 for 24 h. Co-IP was performed by incubating whole-cellular lysates (200 µg) with an anti-HA antibody. **(D)** Mutation of the p38α MAPK phosphorylation site or sites on ULK1 blocks p38α MAPK–induced ULK1–ATG13 complex disruption. HEK293 cells were transfected as indicated and assessed for protein expression by Western blotting (bottom) and for HA-ATG13 and MYC-ULK1 binding by co-IP (top). WB, Western blot. **, $P < 0.01$ versus control; ##, $P < 0.01$ versus p38α. $n = 4$. Error bars show SD.

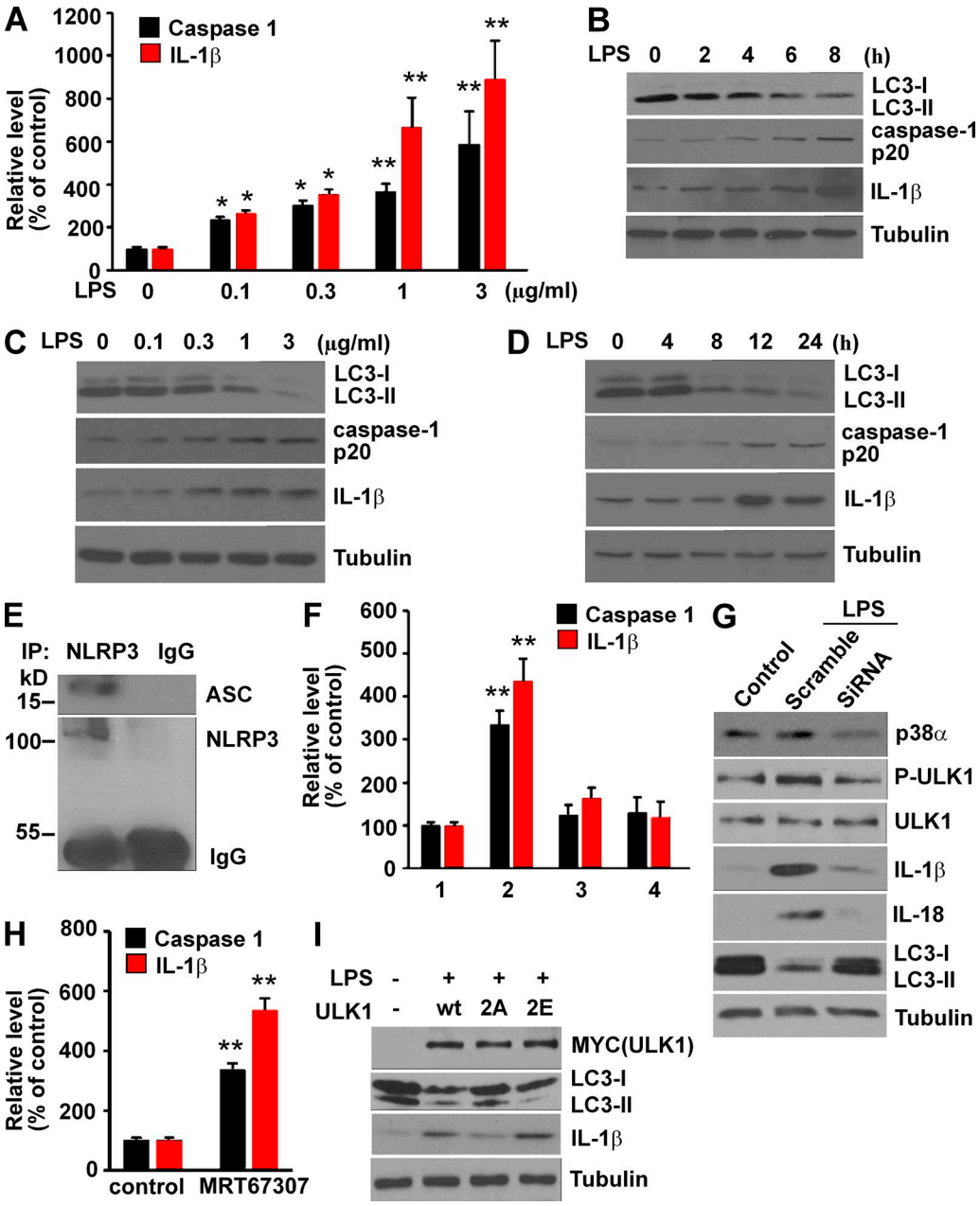

Figure S5. **LPS-induced inflammatory response in BV2 cells and primary microglia correlates closely with a reduction of LC3-II level. (A)** LPS (8 h) induces the release of caspase-1 and IL-1β into culture media in primary microglia. Culture media were analyzed by ELISA after LPS treatment. **(B)** LPS (1 μg/ml) causes a time-dependent reduction of LC3-II and activation of primary microglia. **(C)** LPS causes a dose-dependent reduction of LC3-II and activation of BV2 cells. **(D)** LPS (1 μg/ml) causes a time-dependent reduction of LC3-II and activation of BV2 cells. **(E)** NLRP3 and ASC interact with each other in BV2 cells under basal conditions. Co-IP was performed using anti-NLRP3 antibody and BV2 lysates. **(F)** LPS (8 h; 1 μg/ml) induces the release of caspase-1 and IL-1β into media in primary microglia through p38α MAPK. Culture media from cells treated as in Fig. 6 C was analyzed by ELISA. **(G)** Knockdown of p38α MAPK blocks LPS (1 μg/ml)-induced activation of primary microglia. **(H)** Inhibition of ULK1 enhances the release of caspase-1 and IL-1β into media from primary microglia. **(I)** The expression of ULK1 mutants modulates LPS (1 μg/ml)-induced changes of LC3-II and IL-1β. Primary microglia transduced with recombinant lentivirus expressing WT or mutant ULK1 (S504A/S757A and ULK1/2A or S504E/S757E and ULK1/2E) were blotted. *, $P < 0.05$; **, $P < 0.01$ versus control.

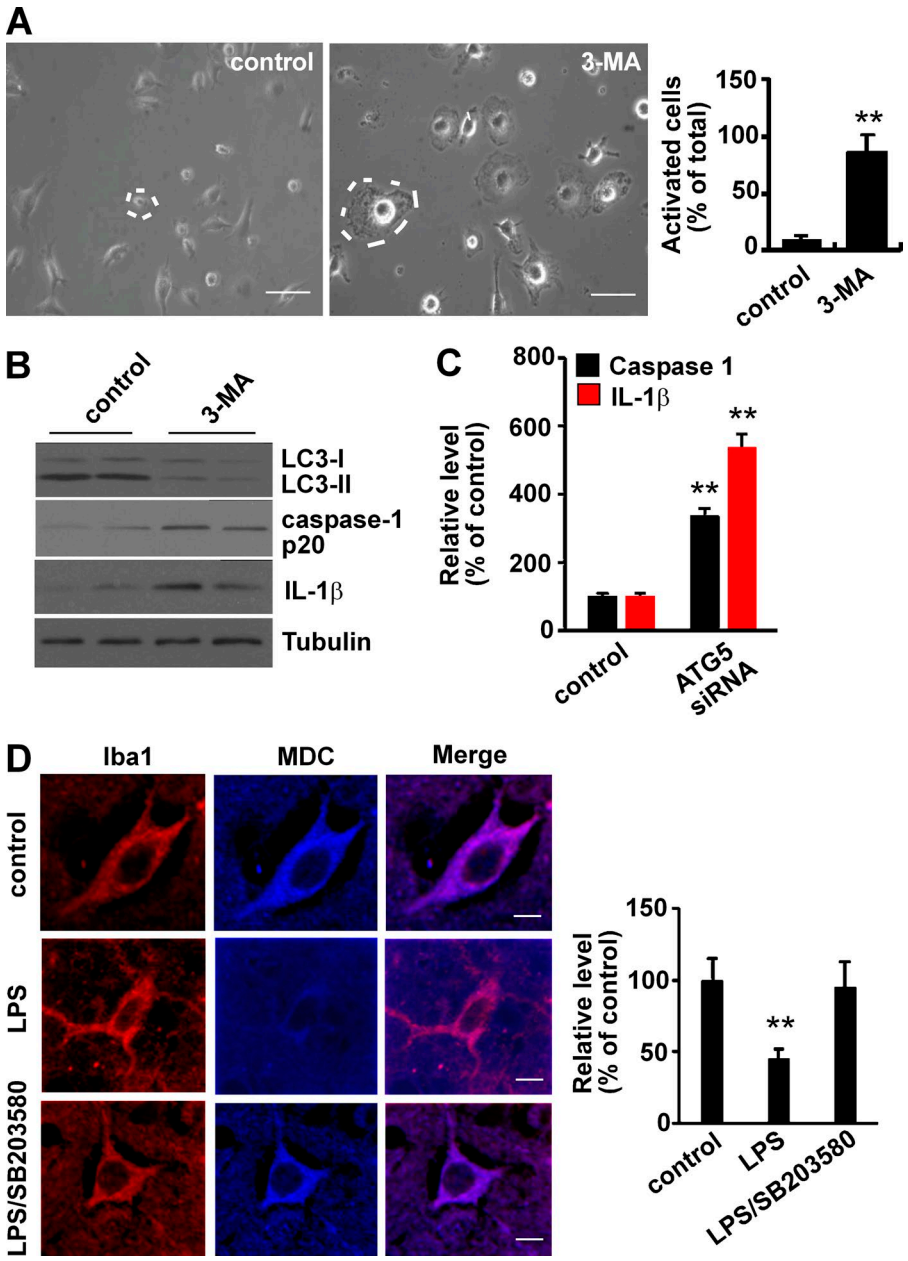

Figure S6. **Inhibition of autophagy induces inflammation in primary microglia and in vivo. (A)** Inhibition of autophagy with 3-MA induces morphological changes in cultured primary microglia. Primary microglia were treated with 3-MA (5 mM) for 12 h and scored for process retraction and cell body enlargement. Dashed lines indicate cell outlines. Bars, 40 µm. *n* = 100. **(B)** Inhibition of autophagy with 3-MA causes inflammatory response. Primary microglia were treated with 3-MA (5 mM) for 8 h and analyzed for LC3 level, caspase-1 activation, and IL-1β production. **(C)** ATG5 knockdown causes inflammatory response. Media from primary microglia treated as in Fig. 7 B were analyzed for caspase-1 and IL-1β. **(D)** LPS reduces the number of autophagosomes in the mouse brain. LPS (5 µg/side; I.C.V.) was injected into 1-mo-old CD1 mice. SB203580 (2 mg/animal; i.p.) was injected 2 h before and 0 h after LPS admission. 24 h later, MDC (1.5 mg/kg; i.p.) was injected. 2 h later, whole animals were perfused with saline and 4% paraformaldehyde for MDC imaging of the cortical region. Bars, 20 µm. **, P < 0.01 versus control. Experiments were repeated three times. Error bars show SD.